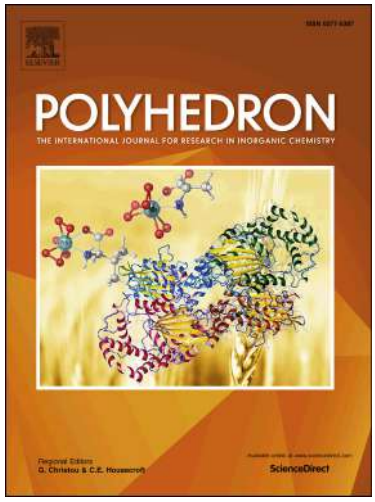

Synthesis of a new pyridinyl thiazole ligand with hydrazone moiety and its cobalt(III) complex: X-ray crystallography, *in vitro* evaluation of antibacterial activity

Pradip Bera, Paula Brandão, Gopinath Mondal, Harekrishna Jana, Abhimanyu Jana, Ananyakumari Santra, Pulakesh Bera

PII: S0277-5387(17)30442-4
DOI: http://dx.doi.org/10.1016/j.poly.2017.06.024
Reference: POLY 12705

To appear in: *Polyhedron*

Received Date: 19 April 2017
Accepted Date: 16 June 2017

Please cite this article as: P. Bera, P. Brandão, G. Mondal, H. Jana, A. Jana, A. Santra, P. Bera, Synthesis of a new pyridinyl thiazole ligand with hydrazone moiety and its cobalt(III) complex: X-ray crystallography, *in vitro* evaluation of antibacterial activity, *Polyhedron* (2017), doi: http://dx.doi.org/10.1016/j.poly.2017.06.024

Synthesis of a new pyridinyl thiazole ligand with hydrazone moiety and its cobalt(III) complex: X-ray crystallography, *in vitro* evaluation of antibacterial activity

Pradip Bera[a], Paula Brandão[b], Gopinath Mondal[a], Harekrishna Jana[c], Abhimanyu Jana[a], Ananyakumari Santra[a], Pulakesh Bera*[a]

[a]*Post Graduate Department of Chemistry, Panskura Banamali College, Vidyasagar University, Midnapore (E), West Bengal-721152, India*

[b]*Department of Chemistry, CICECO, University of Aveiro, 3810-193 Aveiro, Portugal*

[c]*Department of Microbiology, Panskura Banamali College, Vidyasagar University, Midnapore (E), West Bengal-721152, India*

Abstract: The present work report the synthesis, structural characterization and *in vitro* antibacterial studies of 4-(4-methoxy phenyl)-2-(2-(1-pyridine-2-yl)ethylidene) hydrazinyl)thiazole bromide (HL·Br) and its cobalt(III) complex, $[CoL_2]ClO_4$. HL·Br crystallizes in a space group Pbca in a nearly planar structure and the crystal structure of complex shows a $Co^{III}N6$ coordination geometry in which each L shows N,N,N-donor binding modes. Solution magnetic susceptibility measurement of $[CoL_2]ClO_4$ by modified Evan's method confirms the low spin diamagnetic nature of the cobalt(III) complex. New compounds were screened for their antibacterial studies against gram positive bacteria including *Staphylococcus aureus, Streptococcus fecalis* and *Bacillus subtilis* and gram-negative bacteria including *Escherichia coli, Pseudomonas aeruginosa, Salmonella Typhi, Klebsiella pneumonia* and *Proteus vulgaris.* Both the compounds show very stronger growth inhibition activity against gram negative bacteria than gram positive bacteria. Present study shows that HL·Br has maximum antibacterial activity against *E.coli* (25±0.2 mm) and S.typhi (28±0.7 mm) at an MIC of 200 µg/mL and 50 µg/mL respectively, showing greater MIC values than the standard antibiotic ciprofloxacin (8 µg/mL against *E.coli and* 10 µg/mL against *S.typhi*).

Key words: Thiazole, Hydrazone, Co(III)complex, Crystallography, Antibacterial activity.

1. Introduction

Thiazole ring system is a pharmacophore found in major natural and biologically active compounds [1–7]. A vast number of 1,3-thiazole-based compounds were considered as ligands in the biology and chemistry due to their ability to coordination various metal ions. The coordination ability of 1,3-thiazole-based ligands is attributed to the presence of sulphur and nitrogen in the five-membered thiazole ring but mode of coordination can be enhanced by structural modification and introduction of a variety of substituents with suitable donors. A series of 2,4-substituted thiazole derivatives containing substituted pyrazole moiety was synthesized and shown to be better antibacterial activities against *S. aureus* bacteria as compared to the standard drug Ceftriaxone [8]. Recently research on pyridine and thiazole containing neonicotinoids have also been substantiated because of their high target specificity with relatively low risk for non-target organism and in the environment [9]. The 2-D and 3-D model cell culture were performed with pyridine-thiazole core compounds to screen the antitumor activity against human breast cancer MCF-7. Results revealed that the pyridine-thiazole compounds are more potent inducer of cell death than cisplatin after 24 hours incubation [10]. In this context, a class of thiazoles e.g., (thiazole-2-yl) hydrazones are important for showing antituberculosic, antifungal, antibacterial, antiparasitic, antioxidant and anticancer activities [11], and potent inhibitory activities against human monoamine oxidase B and histonacetyltransferase [12–14]. The hydrazone derivatives can be prepared by Hantzsch's reaction of thiosemicarbazones and α−haloarylcabonyl compounds [15,16]. P. Chimenti *et al.* synthesized a series of 4-substituted-2-thiazolyl hydrazone derivative and proved the inhibitory activity of human monoamine oxidase, hMAO-A/B isoforms [12]. It was concluded that the substitution at

C4 of the thiazole ring enhanced selective potentiality as hMAO-B inhibitor with IC_{50} values in the nanomolar range [12]. In the search for new anti-infective agents, we took into account the importance of a thiazole ring, which is one of the possible molecular complications of thiosemicarbazone moiety. The contribution of the presence of a hydrazine moiety is also important, as reported before [15,16]. It was well documented that the metal complexes of these heterocyclic ligands are more effective showing various biological activities. Apart from being a chemical element essential for normal metabolic function and a key substituent in vitamin B12, cobalt was chosen as the central metal ion since its complexes often possess higher activities than cisplatin (CDDP)[II] [17]. In the present study, we prepared one pyridine-thiazolyl compound with hydrazone moiety, (E)-4-(4-methoxy phenyl)-2-(2-(1-pyridine-2-yl) ethylidene) hydrazinyl) thiazole bromide (HL.Br) and its cobalt complex to screen their antibacterial activities.

2. Experimental

2.1. Materials

Thiosemicarbazide (99%), 2-acetyl pyridine (99%) and 2-bromo-4-methoxyacetophenon were obtained from Aldrich Chemical Company. Cobalt(II) perchlorate hexahydrate was obtained from Merck chemical company. All solvent (reagent grade) were obtained from commercial suppliers and used after distillation.

2.2. Preparation of Ligand (E)-4-(4-methoxy phenyl)-2-(2-(1-pyridin-2-yl) ethylidene) hydrazinyl) thiazole bromide (HL·Br)

The target ligand HL·Br was prepared by the condensation of 2-bromo-4-methoxyacetophenone and 2-acetylpyridine thioscmicarbazone. The methanolic solution of 2-bromo-4-

methoxyacetophenone (10 mmol, 2.29 gm) is added drop wise in a methanolic solution of 2-acetylpyridine thioscmicarbazone (10mmol, 1.942 gm) [15] with constant stirring at room temperature. The stirring is continued for 4 hours keeping the reaction temperature at 80–90 °C. A yellowish orange precipitate was obtained which was filtered off and washed 2 to 3 times with aqueous methanol. Single crystal suitable for X-ray crystallography were obtained by slow evaporation of methanolic solution of HL·Br. Yield: 3.124 gm (73.79%) Anal. calcd for $C_{17}H_{19}BrN_4O_2S$ (%) C, 48.35; H, 4.30; Br, 18.92; N, 13.27; O, 7.58; S, 7.59 Found C, 48.19; H, 4.48; N, 13.22; S, 7.55, O, 7.55; Br, 18.87. ^{1}H NMR (DMSO-d_6) δ (in ppm) : 2.41-2.49, (s, 3H at C7), 3.74–3.81 (s, 3H at C17), 6.96 and 6.98 (d, 2H at C13 and C15, $^3J_{13,12}$= $^3J_{15,16}$=8.0Hz); 7.23 (s, 1H at C9), 7.79 and 7.81 (d, 2H at C12 and C16, $^3J_{12,13}$=$^3J_{16,15}$=8.0Hz), 7.56 (m, 1H at C2), 8.1 (m, 2H at C3 and C4), 8.645 (m, 1H at C1).

2.3. Preparation of complex

20 mL methanolic solution containing HL·Br (1mmol, 0.42 gm) and $Co(ClO_4)_2.6H_2O$ (1mmol, 0.36 gm) was stirred in open air for one hour at room temperature. The resulting solution is refluxed in water bath for three hours. The colour of the solution changes light yellow to deep reddish brown. The resultant solution was filtered and the filtrate was allowed to keep for slow evaporation. The brown black crystals were obtained. Yield 70%. Anal. calcd for $C_{34}H_{30}ClCoN_8O_6S_2$(%) C, 57.70; H, 4.56; N, 15.83; S, 9.06. Found C, 57.67; H, 4.52; N, 15.91; S, 9.21.

2.4. Characterization

Single crystal X-ray diffraction data for ligand and complex were collected with monochromated Mo-Kα radiation (λ = 0.71073 Å) on a Bruker Kappa Apex-II diffractometer, equipped with a

CCD area detector at low temperatures. Several scans in φ and ω directions were made to increase the number of redundant reflections and were averaged during the refinement cycles. Data processing for all the complexes were performed using Bruker Apex-II suite. Reflections were then corrected for absorption, inter-frame scaling, and other systematic errors with SADABS [18]. All the structures were solved by the direct methods and all non-hydrogen atoms were refined anisotropically by the full-matrix least squares based on F^2 using the SHELXL-97 [19]. The hydrogen atoms were isotropically treated using a riding model with their isotropic displacement parameters depending on the parent atoms. A summary of the crystallographic data and refinement parameters are given in Table 1. The molar conductance of 10^{-3} (M) solution of the metal complexes in DMSO were measure at 30 °C using a Thermo Orion model 550A conductivity meter and a dip-type cell with platinized electrode. The elemental analysis (C, H, N, and S) of the complex was performed using a FISONS EA-1108 CHN analyzer. UV-Visible absorption spectra of the samples were recorded on a Perkin Elmer Lambda 35 spectrophotometer in the wavelength range region 200–800 nm at room temperature. ^{1}H-NMR spectrum of ligand was recorded using a JEOL JNM-ECZ 400S/L1 400 MHz NMR spectrometer. Magnetic susceptibility measurement of complex in solution were carried out using a Bruker Spectrometer 400 MHz following a standard NMR methodology using solution of $CDCl_3$ and tertiary butanol (v/v 20). The solution was prepared by dissolving 1.10 mg of sample (M. wt.= 805.16) in 485 µL $CDCl_3$ and 15 µL of t-BuOH. A solution of 260 µL$CDCl_3$ and 8 µL t-BuOH was prepared for the co-axial capillary filling for the Evan's method [20]. The equation for determining the mass susceptibility (χ_g in cm^3/g) using NMR instrumentation where the external magnetic field is coaxial with the sample tube is given below:

$$\chi_g = -[3\Delta f/4\pi F_c] + \chi_0 + [\chi_0(d_0-d_s)/c]$$

where Δf is the observed frequency shift of the reference resonance (e.g., tertiary butanol signal), F is the fixed probe frequency in Hz of the NMR spectrophotometer, χ_0 is the mass susceptibility of the solvent, c is the concentration in grams of the complex per $cm^3$of solution, and d_0 and d_s are the respective densities (g/cm^3) for the solvent and solution. The last two terms in the equation correct for the solvent's diamagnetic contribution by taking into account the change in its density after adding the solute. In this study the complex concentration was less than 10 mM which allows for the solution density (d_s) to be approximated by d_0+m; hence, the mass susceptibility equation simplifies as $\chi_g = -[3\Delta f/4\pi F_c]$ [21]. The calculation of μ_{eff} is sensitive to the concentration of the dissolved paramagnetic material. The molar susceptibility (χ_g in cm^3/mol) for each complex was determined by multiplying χg by the molar mass (g/mol). The effective magnetic moment (μ_{eff}) in Bohr magneton was calculated from paramagnetic molar susceptibility (χg) using the relationship $\mu_{eff} = 2.828(\chi g.T)^{1/2}$ where T is the temperature in Kelvin. The predominant source of error was in the determination of solution concentration due to the small samples prepared (0.5 mL).

Cyclic voltammetric experiments were performed at room temperature in acetonitrile solvent using tetra butyl ammonium perchlorate as a supporting electrolyte on a CH Instrument electrochemical workstation model CHI630E. The conventional three-electrode assembly is comprised of a platinum working electrode, a platinum wire auxiliary electrode and a Ag/AgCl reference electrode. UV–Vis absorption spectra of the samples were recorded on a Perkin Elmer Lambda 35 spectrophotometer in the wavelength range region 200–800 nm at room temperature.

2.5. Qualitative antibacterial assays

Antibacterial sensitivity of the ligand and its cobalt complex were tested by the agar well diffusion method using Mueller-Hilton agar media. The agar diffusion method was employed for

the determination of antibacterial activities according to the method described by Chattopadyay [22]. The compounds under investigation were dissolved in methanol to a final concentration of 500 μg/mL. Eight species of pathogenic bacteria namely *Escherichia coli, Klebsiella pneumoniae, Staphylococcus aureus, Streptococcus fecalis, Salmonella typhi, Proteus vulgaris, Pseudomonas aeruginous and Bacillus subtilis* were used to screen the antibacterial activity of the metal complex [23]. Pathogenic bacterial strains were incubated in sterile nutrient broth and incubated at 37 ºC for 24 h. The pathogen were swabbed (Inoculums size was adjusted so as to deliver a final inoculums of approximately 10^6 CFU/mL) on the surface of Mueller-Hilton agar media and petri dishes containing 20 mL of Mueller–Hinton Agar with 100 μL inoculums of bacterial strain and Media was allowed to solidify. Wells were cut into solidified agar media with the help of sterilized cup-borer. 100 μL of each sample solution was poured in the respective wells and the plates including control were incubated overnight at 37 °C for bacteria. The experiment was performed in triplicate under strict aseptic conditions and the antibacterial activity of each compound was expressed in terms of the mean diameter of zone of inhibition (mm) produced by the respective compound.

2.6. Determination of MIC value

Minimum inhibitory concentration was determined using inhibitory concentration in diffusion (ICD) method [24]. The minimal inhibitory concentration (MIC) values, which represent the lowest concentration of the compound that completely inhibits the growth of microorganisms, were determined by a micro-well dilution method [25] The inoculums of each bacterium were prepared and the suspensions were adjusted to 10^6 CFU/mL. For making these dilutions, ligand HL·Br and its cobalt complex were dissolved at a concentrations and diluted in methanol to obtain different concentration as 500 μg/mL, 400 μg/mL, 300 μg/mL, 200 μg/mL, 100 μg/mL,75

μg/mL, 50 μg/mL, 25 μg/mL. 100 μL of compound of different concentration was poured in the respective wells and the plates were incubated for 24 hours at 37 °C. The experiment was performed in triplicate under strict aseptic conditions.

3. Results and discussion

Previously, a series of 2-(pyridine-2-yl)-1,3-thiazoles were prepared via Hanstsch cyclization between 2-pyridine-2-yl)thiosemicarbazones and substituted 2-bromoacetophenones adopting ultrasound condition [15]. These compounds have very similar composition with the present ligand HL·Br except the substitution at 4-position at thiazole moiety. Very recently, *trans* isomer of 2-(2-pyridine-2-ylmethylene)hydrazinyl)-4-(4-tolyl)-1,3-thiazole was structurally characterized [10]. However, we are able to crystallize the organic molecule (L) as bromide salt rather than neutral molecule. Ligand HL·Br was prepared following Hantsch's reaction where equimolecular mixture of 2-acetyl pyridine thiosemicarbazone and 2-bromo-4-methoxy acetophenone were refluxed in methanol (Scheme 1). Preferential crystallization as bromide salt is quite expected when charge of the pyridinium ion of HL was satisfied by the bromide ion. It is worth mentioning that the large size of the bromide ion preferentially stabilized the crystal of HL·Br. It is interesting to note that in a similar reaction condition, the perchlorate salt of L ($HL{\cdot}ClO_4$) was obtained in the presence of excess perchloric acid. The detail structural characterization of $HL{\cdot}ClO_4$ is beyond the scope of this report (CCDC deposition 1530855). The signals obtained in the ^{1}H-NMR spectrum of the ligand were in good agreement with the expected structure (Fig. S1). The signal at δ 2.41-2.49 can be assigned for the three iminomethyl proton on C7 [26]. On the other hand the broad signal in the region δ 4.0-4.5 may be due to the single acidic proton at N3 which is in conjugation with thiazole ring. The doublet peak in the

region δ 6.96 and 6.98 can be assigned for the protons attached to C13 and C15 with J value 8.0 Hz (Scheme 1). Similarly, the doublet peak in the region δ 7.78 and 7.81 ppm correspond to protons attached to C12 and C16, respectively with a J value 8.0 Hz. The J-values indicates that the protons attached to C12 and C13 mutually couple in a same extent with the coupling of protons attached to C15 and C16. Fine spectrum of the complex was obtained in mixed solvent $CDCl_3$ and tert-BuOH without any deformation of the multiplet proton peaks. This indicates that the complex itself is diamagnetic in nature. Slight shifting of the methyl protons of tert-BuOH (Δf=0.04 ppm) in the spectrum of coaxially arranged capillary containing solution of $CDCl_3$ and tert-BuOH(v/v 20) with the complex in the same mixture in the NMR sample tube (Evan's method) gives up very low μ_{eff} value *ca.*1.43 BM confirms the low spin state of cobalt (Fig. S2).

The reaction of HL·Br and $Co(ClO_4)_2.6H_2O$ furnished the complex cobalt(III) complex with composition $[CoL_2](ClO_4)_2$. The aerobic oxidation of cobalt(II) to cobalt(III) is quite expected in the reaction condition. Both ligand and complex were structurally characterized and their antibacterial activities were tested. The low spin nature of the complex, $[CoL_2](ClO_4)_2$ can be attributed by the UV-Vis spectrum where a broad weak absorption band appeared at 470 nm for d-d transition and the high energy absorption band appeared at 344 nm (thiazole to metal CT transition) (Fig. S3).

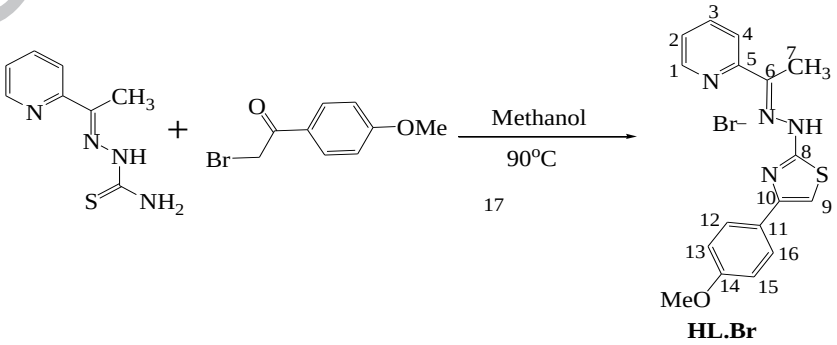

Scheme-1: Synthesis of ligand **HL.Br**

3.1. X-ray crystallography

The X-ray crystal structure of (E)-4-(4-methoxy phenyl)-2-(2-(1-pyridin-2-yl)ethylidene) hydrazinyl)thiazole bromide (HL·Br) and cobalt complex are shown in Figure1 and Figure 2, respectively. Crystal refinement data of HL·Br and complex are summarized in Table 1. The angles between the plane C12-C11-C10 and C11-C10-N4, C10-N4-C8 and N4-C8-N3, C8-N3-N2 and N3-N2-C6, and N2-C6-C5 and C6-C5-N1 are 8.64°, 0.41°, 3.29° and 3.67° respectively, indicate that the molecule is nearly planar. In the thiazole ring, two sufficiently different bonds are found *viz*. C8–N4 (1.308Å) and C10–C9 (1.357Å) clearly indicative of double bond in the aromatic ring system. It is clearly to be shown that the ligand molecule crystallize in a Z-isomeric form with intermolecular H-bonding with bromide and oxygen atom of water of crystallization (Figure 3). Corresponding H-bondings are given in Table 2. The presence of bromide ion in the asymmetric unit is a proof of preferential crystallization as a bromide salt of quaternary pyridinium ion rather than neutral ligand molecule. The bromide group counters balance the quaternary nitrogen and also participate in H-bonding. A detailed analysis of the crystal packing of the ligand shows that the molecules stack into supramolecular chains along the b-axis due to π…π and C–H…O interactions between neighbouring molecules in the stack. The planarity and the solubility of the bromide salt are likely to make it very effective for DNA interaction.

As anticipated, the asymmetric unit of the cobalt(III) complex contains crystallographically independent twin $[Co(L)_2]^+$ octahedral entities. A perspective view of the molecular structure is shown in Figure 4. Selected bond angles and bond lengths are given in the Table 3 and Table 4. The cobalt(III) ion is surrounded by the three different 'N' atoms of ligand (HL·Br). Two

heterocyclic 'N' atoms one from pyridine and another from thiazole coordinate with cobalt(III) along with hydrazinic 'N' atom of ligand forming five membered cyclic rings. The coordination sphere around the Co atom adopts an overall octahedral geometry. Both the participating ligands are in a *mer* configuration. The contributing ligands in the complex may be considered as rigid, quasi-planar and possesses E configuration with respect to the azomethine C=N bond. The NNN planes of the ligands are practically orthogonal with angle near 90° in the complex. Several H-bonding are also present in the lattice. The C8-N3 bond distance in complex with respect to ligand is reduced by *ca*. 0.05 Å indicating double bond formation between C8 and N3. The double bond between C8 and N4 in the ligand is indicated by the low bond distance 1.308 Å, which increases to 1.352Å indicating reduction of electron density on complexation. There are no appreciable changes in the bond distances of the ligand while bonding to cobalt except for the C6-N2 and N1-N2 bond distances. In the free ligand, the C6-N2 and N2-N3 bond lengths are 1.289Å and 1.351Å, respectively. The shortening of C6–N2 bond length in complex with respect to free ligand suggests an increase in the double bond character. The Co–N bond distances in the range 1.86 to 1.99Å were well documented for the spin free diamagnetic cobalt(III) complexes with multi N-donor ligands [27–30]. The distances of Co–N bonds in the present complex are in the range of 1.87Å to 1.93Å which are shorter than the reported Co–N distances [27,28]. The π-acceptor and σ-donor property of thiazole derivative provide a relatively large ligand field splitting energy between the metal localized dπ and dσ* orbitals corresponding to electronic arrangement $t_{2g}^{6}e_{g}^{0}$. Thus effective donation occurs with the approach of the donor atoms along the axes (vacant e_g orbitals) which accounts the shortening of Co–N bonds in the complex.

3.2. Electrochemical study of complex

A study of the electrochemical behavior of a metal complex has an immense role in exploring the chemical and electrochemical reactions and mechanism involving such a molecule. The redox property of a bioactive compound can also give insight into its metabolic facts and biological activities. We studied the electrochemical behavior of the present compound since this category of compound has a wide application in biology and chemistry. The cyclovoltammogram of the complex $[CoL_2]ClO_4$ shows three reduction peaks at –0.83 V (I), +0.56 V (II) and +0.85 V (III) versus Ag/AgCl, saturated KCl, respectively, while there are two oxidation peaks and at –0.45 V (IV) and 0.93 V (V) versus Ag/AgCl, saturated KCl, respectively, at a scan rate 100 mVs^{-1} (Figure 5). The first reduction peak (I) for the cobalt complex corresponds to the reduction of the ligand centre while the second reduction (II) involves the one electron reduction of Co(III) to Co(II). The remaining third reduction peak (III) may be attributed to the reduction of Co(II) to Co(I) species. The predominant single oxidation peak at 0.93 V (V) might be the combination of oxidation processes Co(I)→Co(II) and Co(II)→Co(III). The nature of the reduction and oxidation processes are irreversible which reveals that the complex predominantly contains one kind of species, e.g., Co^{3+} on dissolution.

3.3 Antimicrobial activity

The efficiency of antibacterial effects of any compound (natural or synthetic) depends on the penetration power of the compound to the organisms. The available antibacterial agents target structures and functions or both which are relevant to the organisms to be inhibited. For example, many antibacterial agents inhibit the formation of peptidoglycan, the essential component of the bacterial lipid bilayer of cell membrane and cell wall.

Many classes of antibacterial agents are protein synthesis inhibitors such as amino glycosides, macrolides and tetracyclines; topoisomerase inhibitors such as fluoroquinolones; and metabolic

pathway inhibitors such as trimethoprim-sulfamethoxazole. The compounds under investigation showed very stronger growth inhibition activity against gram negative bacteria than gram positive bacteria. Figure 6 represents that HL·Br has maximum antibacterial activity against *E.coli* (25 mm) and *S.typhi* (28 mm) (Table 5) at an MIC of 200 µg/mL and 50 µg/mL, respectively showing greater MIC values (Fig. S4) than standard antibiotic (ciprofloxacin) with values 8 µg/mL against *E.coli* and 10 µg/mL against *S.typhi* (Table 6 and Table 7).

From the study it is revealed that HL·Br shows better antibacterial activity than its cobalt complex. The higher antibacterial property of HL·Br can be attributed to the planar structure and the good solubility in methanol. The planar structure preferentially penetrates to the cells of microorganism and the cell binding activity is facilitated by the good solubility of the pyridinium ion of HL·Br. Additionally, the hydrolysis of HL·Br increases the acidity of the medium causing the higher antibacterial activity than corresponding cobalt complex. However, the complex $[CoL_2]ClO_4$ produces $[CoL_2]^+$ and ClO_4^- on dissolution. The 3D structure of $[CoL_2]^+$ counter balanced by ClO_4^-, has less penetration to the bacterial cell and does not change pH significantly. This fact suggests the lesser antibacterial activity of complex than the ligand.

4. Conclusion

A thiazolyl pyridinium bromide molecule (HL·Br) and its cobalt(II) complex are synthesized and structurally characterized. The ligand (HL.Br) having rigid, quasi E configuration forms low spin diamagnetic $[CoL_2]ClO_4$ complex. The asymmetric unit of the cobalt(III) complex contains crystallographically independent twin $[Co(L)_2]^{2+}$ octahedral entities. The coordination sites of the complex are occupied by two heterocyclic 'N' atoms (one from pyridine and another from thiazole) and one hydrazinic 'N' atom of each ligand molecule forming five membered cyclic rings. Both the ligand and complex are fairly soluble in aqueous methanol and used in culture medium for biological experiments. The compounds showed stronger growth inhibition activity against gram negative bacteria than gram positive bacteria. The ligand shows better antibacterial activity due to its fair solubility in aqueous medium than corresponding cobalt complex. Further researches on thiazole derivatives with hydrazone moiety need to be explored for better understanding of biological activities.

Acknowledgement

We gratefully acknowledge to Council for Scientific and Industrial Research (CSIR) for the project grant (No.1(2858)/16/EMR-II) and also to University Grants Commission (UGC), Government of India for the extension of the project [F 42-280/2013(SR)]. We are also thankful to Dr. Anangamohan Panja, Department of Chemistry, Panskura Banamali College for fruitful discussion on crystallography.

Appendix A. Supplementary data

CCDC 1528638, 1528639 and 1530855 contain the supplementary crystallographic data for HL·Br, $CoL_2.ClO_4$ and HL·ClO_4, respectively. These data can be obtained free of charge via

http://www.ccdc.cam.ac.uk/conts/retrieving.html, or from the Cambridge Crystallographic Data Centre, 12 Union Road, Cambridge CB2 1EZ, UK; fax: (+44) 1223-336-033; or e-mail: deposit@ccdc.cam.ac.uk.

References

1. C.S. Feng, W. Yan, L.V.J. Song, G.L.V. Damu, C.H. Zhou, Scientia Sinica Chimica 42 (2012) 1105−1131.

2. L.M.T. Frija, A.J.L. Pombeiro, M.N. Kopylovich, Coord. Chem. Rev 308 (2016) 32−55.

3. W.T. Li, D.R. Hwang, J.S. Song, C.P. Chen, T.W. Chen, C.H. Lin, J.J. Chuu, T.W. Lien, T.A. Hsu, C.L. Huang, H.Y. Tseng, C.C. Lin, H.L. Lin, C.M. Chang, Y.S. Chao, C.T. Chen, Invest New Drugs 30 (2012) 164–175.

4. A. Jessica. Edwards, M. Megan. Kemski, A. Chad, Rappleye Antimicrobial Agents and Chemotherapy 574 (2013) 349–4359.

5. C.Y. Tsai, M. Kapoor, Y.P. Huang, H.H. Lin, Y.C. Liang, Y.L. Lin, S.C. Huang, W.N. Liao, J.K. Chen, J.S. Huang, M.H. Hsu, Molecules. 21 (2016) 145-153.

6. M.K. Kathiravan, A.B. Salake, A.S. Chothe, P.B. Dudhe, R.P. Watode, M.S. Mukta, S. Gadhwe, Bioorg. Med. Chem. 20 (2012) 5678–5698.

7. Y. Bansal, O. Silakari, Bioorg. Med. Chem. 20 (2012) 6208–6236.

8. A.M. Vijesh, A.M. Isloor, V. Prabhu, S. Ahmad, S. Malladi, Eur. J Med. Chem. 45 (2010) 5460-5464.

9. P. Jeschke, Bioactive Heterocyclic compounds class (2012) Agrochemicals, First Ed., Wiley-Vchverleg GmbH & co.

10. H. Elshaflu, S. Bjelogrlic, C.D. Muller, T.R. Todorovic, M. Rodic, A. Marinkovic, N.R. Filipovic, J Coord. Chem. 69 (2016) 3354–3366.

11. S. Rollas , S.G. Küçükgüzel, Molecules 12(8) (2007) 1910–1939.

12. P. Chimenti, A. Petzer, S. Carradori, M. D'Ascenzio, R. Silvestri, S. Alcaro, F. Ortuso, J.P. Petzer, D. Secci, Eur. J. Med. Chem. 66 (2013) 221–227.

13. F. Chimenti, E. Maccioni, D. Secci, A. Bolasco, P. Chimenti, A. Granese, O. Befani, P. Turini, S. Alcaro, F. Ortuso, M.C. Cardia, S. Distinto, J. Med. Chem. 50 (2007) 707–712.

14. F. Chimenti, B. Bizzarri, E. Maccioni, D. Secci, A. Bolasco, P. Chimenti, R. Fioravanti, A. Granese, S. Carradori, F. P. Tosi, Ballario, S. Vernarecci, P. Filetici J. Med. Chem. 52 (2009) 530–536.

15. M.V.O. Cardoso, L.R.P. Siqueira, E.B. Silva, L.B. Costa, M.Z. Hernandes, M.M. Rabello, R.S. Ferreira, L.F. Cruz, D.R.M. Moreira, V.R.A. Pereira, M.C.A.B. Castro, P.V. Bernhardt, A.C.L. Leite Eur. J. Med. Chem. 86 (2014) 48–59.

16. M.B. Ferrari, F. Bisceglie, G. Pelosi, P. Tarasconi, R. Albertini, P.D. Aglio, S. Pinelli, A. Alberta Bergamo, G. Gianni Sava J Inorg. Biochem. 98 (2004) 301–312.

17. C.R. Munteanu, K. Suntharalingam, Dalton Trans. 44 (2015) 13796−13808.

18. G.M. Sheldrick, SADABS, University of Göttingen, Germany, 1996.

19. G.M. Sheldrick, SHELXL-97, Crystal Structure Refinement Program, University of Göttingen, 1997.

20. D.F. Evans, Proc. Chem. Soc. (1958) 115–117.

21. M.L. Naklicki, C.A. White, L.L. Plante, C.E. Evans, R.J. Crutchley, Inorg. Chem. 37 (1998) 1880−1885.

22. D. Chattopadhyay, J Antimicrob. Chemother. 42 (1998) 83–85.

23. A. Nostro, Lett Appl Microbiol 30(1) (2000) 379−384.

24. V. Guerin-Faublee, M.L.D. Muller, M. Vigneulle, J.P. Flandrois, Vet Microbiol 51 (1996) 137−149.

25. D. Wade, A. Silveira, L. Rollins-Smith, T. Bergman, J. Silberring, H. Lankinen, Acta Biochim Pol 48 (2001) 1185−1189.

26. R. Benassi, A. Benedetti, F. Taddei, R. Cappelletti, D. Nardi, A. Tajana,. Org. Mag. Resonance 20 (1982) 26–30.

27. J.G. Tojala, A.G. Oradb, A.A. Dovazc, J.L. Serrad, M.K. Urtiagae, M.I. Arriortuae, T. Rojo, J. Inorg. Biochem. 84 (2001) 271–278.

28. A. Castineiras, D.X. West, H. Gebremedhin, T.J. Romack, Inorg. Chim. Acta 216(1994) 229–236.

29. K. Ghosh, K. Harms, S. Chattopadhyay, Polyhedron, 123(2017) 162–175.

30. N. Damme, V. Zaliskyy, A.J. Lough, M.T. Lemaire, Polyhedron 89(2015)155-159.

Tables and Figures

Table 1. Crystal data and structure refinements for HL·Br and $[CoL_2]ClO_4$.

Table 2. Hydrogen bond parameters (Å,°) for HL·Br.

Table 3. Selected bond angles of HL·Br and $[CoL_2]ClO_4$.

Table 4. Selected distance [Å] of the ligand HL·Br and $[Co(L_2)]ClO_4$.

Table 5. Antimicrobial activity of specific concentration (500 µg/ml) of different synthetic compounds compared with control by agar well diffusion method.

Table 6. MIC (Minimum Inhibitory Concentration) value of HL·Br against most sensitive bacteria.

Table 7. MIC (Minimum Inhibitory Concentration) value of $[CoL_2]ClO_4$ complex against most sensitive bacteria.

Fig. 1. Molecular structure of HL·Br showing the atom numbering scheme. Ellipsoids are drawn at the 50% probability level.

Fig. 2. Molecular structure of complex $[CoL_2]ClO_4$ showing the atom numbering scheme. Ellipsoids are drawn at the 50% probability level.

Fig. 3. Packing diagram and 1D hydrogen bonded supramolecular chain along b-axis of ligand HL·Br.

Fig. 4. Molecular twin structure of complex $[CoL_2]ClO_4$.

Fig. 5 Cyclic voltammograms of $[CoL_2]ClO_4$ in acetonitrile solution using a platinum working electrode in the presence of tetraethylammonium perchlorate as a supporting electrolyte at ambient temperature with scan rate 100 mV s^{-1}.

Fig. 6 Inhibition zone of ligand HL·Br and Complex $CoL_2.ClO_4$ against *E.coli*, *Pseudo Monas* and *S. typhi* bacteria.

Table 1.Crystal data and structure refinements for HL·Br and $[CoL_2]ClO_4$.

Parameter	**HL·Br**	**$[CoL_2]ClO_4$**
Formula	$C_{17}\ H_{19}\ Br\ N_4\ O_2\ S$	$C_{34}\ H_{30}Cl\ Co\ N_8\ O_6\ S_2$
Mol. Wt.	423.33	805.16
Crystal System	orthorhombic	monoclinic
Space group	*Pbca*	*C2/c*
T(K)	150(2)	150(2)
a(Å)	14.8195(8)	35.5209(19)
b(Å)	13.7644(9)	22.0664(11)
c(Å)	17.7186(11)	18.0357(9)
α(°)	90	90
β(°)	90	103.906
γ(°)	90	90
V(A^3),Z	3613.3(4), 8	13722.4(12),8
D_{cale}(g cm^3)	1.556	1.559
Absorption Cofficient(mm^{-1})	2.409	0.759
F(000)	1728.0	6624.0
F(000')	1727.26	6638.21
h,k,l(max)	18,17,21	44,27,22
R_1	0.0320	0.0587
wR_2	0.0767(3692)	0.1743(14186)
2θ(maximum)	26.389	26.582

Table 2. Hydrogen bond parameters (Å,°) for HL·Br.

HL·Br- H bond parameters					
D– H····A	D– H(Å)	H····A(Å)	D····A(Å)	D– H····A(°)	Symmetry operation on A
N4····H1B– O1	2.122	0.780	2.876	172.3	xyz
Br····H3A– N3	2.522	0.887	3.383	163.7	X, 1.5-y, 1/2+z
Br····H1A– O1	2.437	0.889	3.323	174.3	xyz
O1····H1C– N1	1.770	0.912	2.661	165.1	xyz

Table 3. Selected bond angles of HL·Br and $CoL_2.ClO_4$.

HL· Br				**$CoL_2.ClO_4$**			
Atom-1	**Atom-2**	**Atom-3**	**Angle(°)**	**Atom-1**	**Atom-2**	**Atom-3**	**Angle (°)**
N3	N2	C6	118.90	N1	Co	N2	81.89
N2	N3	C8	117.70	N2	Co	N4	81.84
C8	N4	C10	109.65	N5	Co	N6	82.62
N1	C5	C6	118.15	N6	Co	N8	80.96
N2	C6	C5	113.89	N2	Co	N8	102.85
S	C8	N3	118.91	N2	Co	N5	93.98
S	C8	N4	115.97	N1	Co	N6	97.00
N3	C8	N4	125.11	N1	Co	N8	92.66
N4	C10	C11	119.30	N1	Co	C5	89.66
C10	C11	C16	122.37	N4	Co	N8	91.12
				N4	Co	N5	91.17
				N4	Co	N6	99.22

Table 4. Selected distance [Å] of the ligand HL·Br and $[Co(L_2)]ClO_4$.

HL·Br			**$[Co(L_2)]ClO_4$**		
Atom 1	**Atom 2**	**Length (Å)**	**Atom 1**	**Atom 2**	**Length(Å)**
S	C8	1.726(2)	Co	N1	1.9260
S	C9	1.720(3)	Co	N2	1.8805
C9	C10	1.357(4)	Co	N4	1.9384
C5	C6	1.467(3)	Co	N5	1.9298
N1	H1C	0.91(3)	Co	N6	1.8747
N1	C1	1.335(3)	Co	N8	1.9378
N1	C5	1.350(3)	N6	C23	1.3037
N2	N3	1.351(3)	N2	N3	1.3606
N2	C6	1.289(3)	N6	N7	1.3607
N3	H3A	0.89(3)	N5	C22	1.3646
N3	C8	1.377(3)	N3	C8	1.3297
N4	C8	1.308(3)	N4	C8	1.3527
N4	C10	1.398(3)	N7	C25	1.3433
C1	H1	0.949	N8	C25	1.3361
O2	C14	1.374(3)	N8	C27	1.4013

Table 5. Antimicrobial activity of specific concentration (500 µg/ml) of different synthetic compounds compared with control by agar well diffusion method.

	Zone of inhibition (mm) against bacteria							
	E.coli mean±SD	*S.aureus* mean±SD	*B.subtilis* mean±SD	*P.aeruginosa* mean±SD	*S.fecalis* mean±SD	S.typhi mean±SD	K.pneumoniae mean±SD	P.vulgaris mean±SD
HL·Br	25±0.2	24±0.1	23±0.2	23±0.1	23±0.9	28±0.7	22±0.7	24±0.5
Control	6.0	6.0	6.0	6.0	6.0	6.0	6.0	6.0
$[CoL_2]ClO_4$	16±0.1	6.0	6.0	12±0.2	6.0	15±1.0	6.0	6.0
Control	6.0	6.0	6.0	6.0	6.0	6.0	6.0	6.0

Table 6. MIC (Minimum Inhibitory Concentration) value of HL·Br against most sensitive bacteria.

Name of bacteria	Concentration(µg/ml)	Antimicrobial zone(mm)
S.typhi	500	14±0.1
	400	13±0.1
	300	12±0.1
	200	11±0.1
	100	11±0.1
	75	10±0.1
	50	9±0.1
	25	-
E.coli	500	17±0.1
	400	14±0.1
	300	13±0.1
	200	10±0.1
	100	-
	75	-
	50	-
	25	-

Table 7. MIC (Minimum Inhibitory Concentration) value of $[CoL_2]ClO_4$ complex against most sensitive bacteria.

Name of bacteria	Concentration(µg/ml)	Antimicrobial zone(mm)
S.typhi	300	16±0.1
	200	14±0.1
	100	11±0.1
	75	7±0.1
	50	-
	25	-
E.coli	300	14±0.1
	200	12±0.1
	100	9±0.1
	75	-
	50	-
	25	-

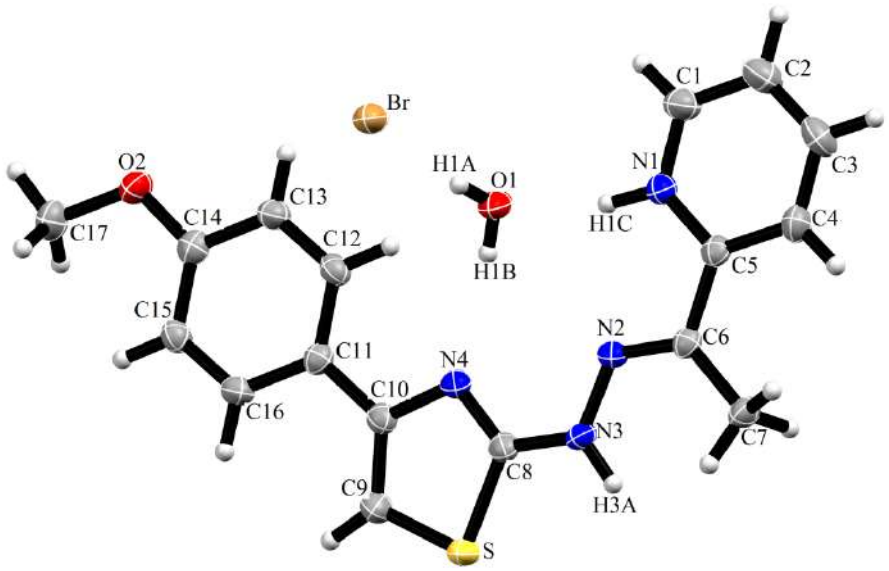

Fig. 1. Molecular structure of HL·Br showing the atom numbering scheme. Ellipsoids are drawn at the 50% probability level.

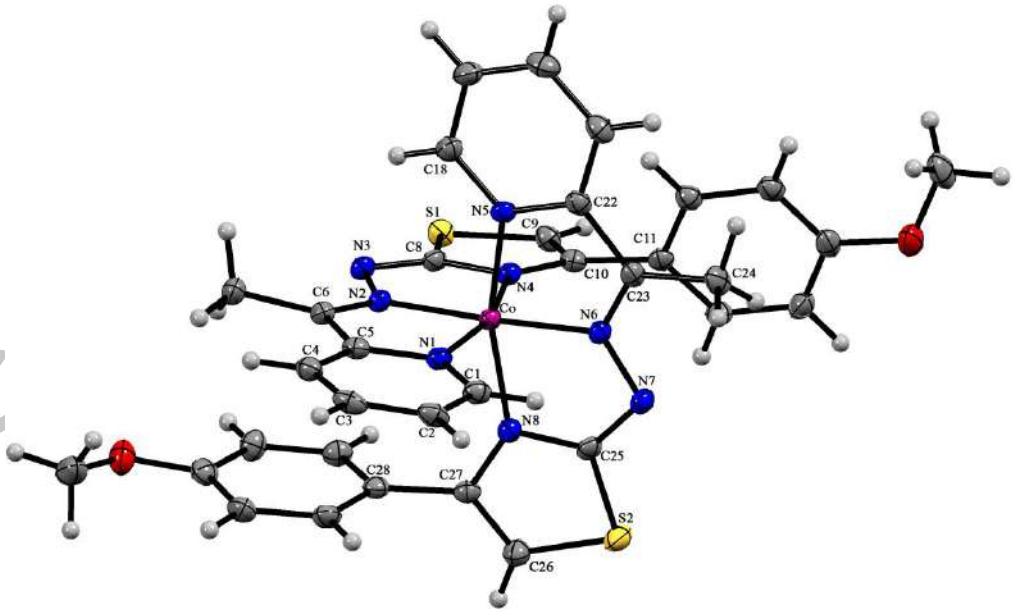

Fig. 2. Molecular structure of complex $[CoL_2]ClO_4$ showing the atom numbering scheme. Ellipsoids are drawn at the 50% probability level.

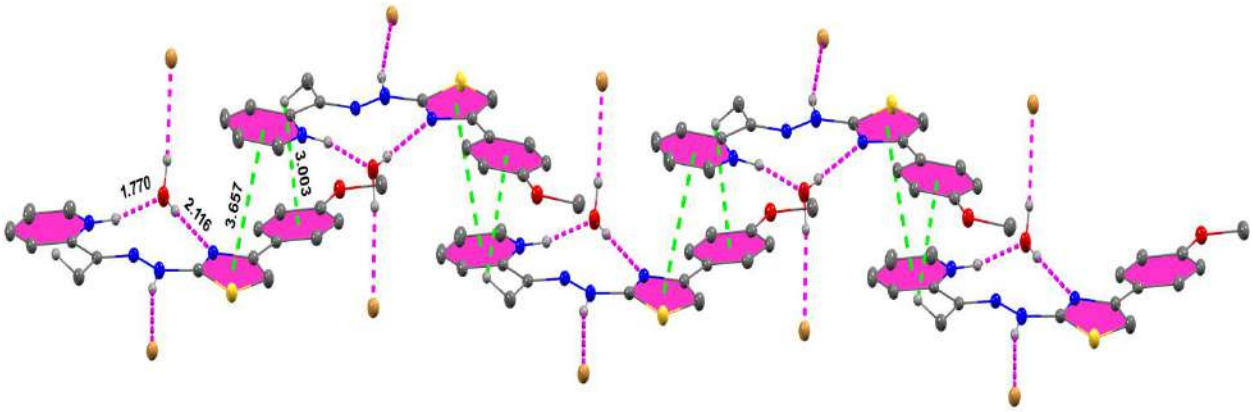

Fig. 3. Packing diagram and 1D hydrogen bonded supramolecular chain along b-axis of ligand HL·Br.

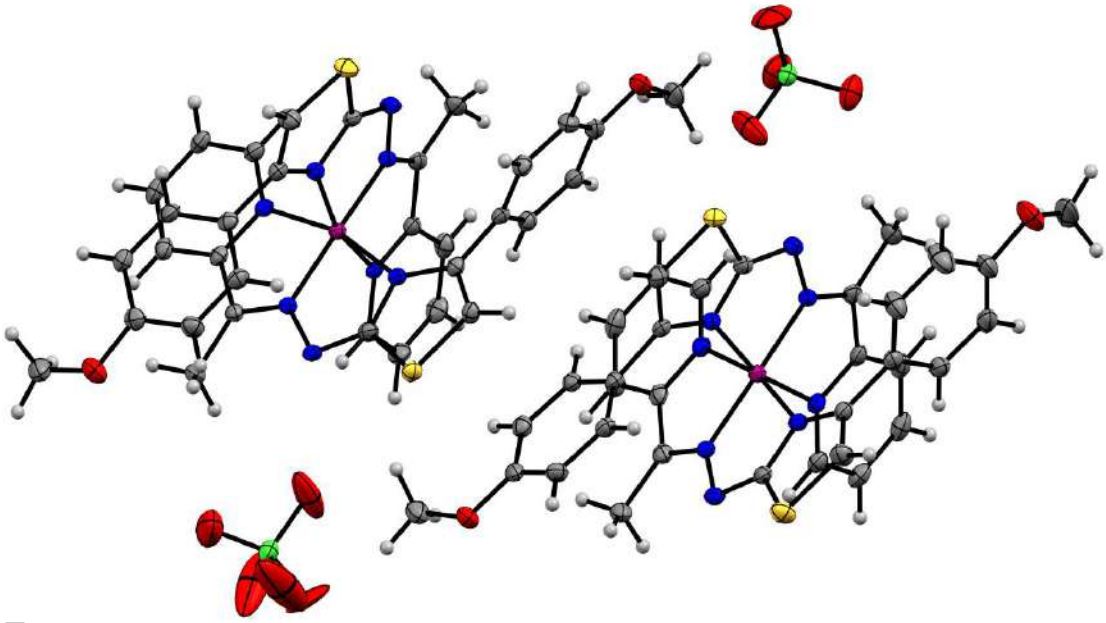

Fig. 4. Molecular twin structure of complex $[CoL_2]ClO_4$.

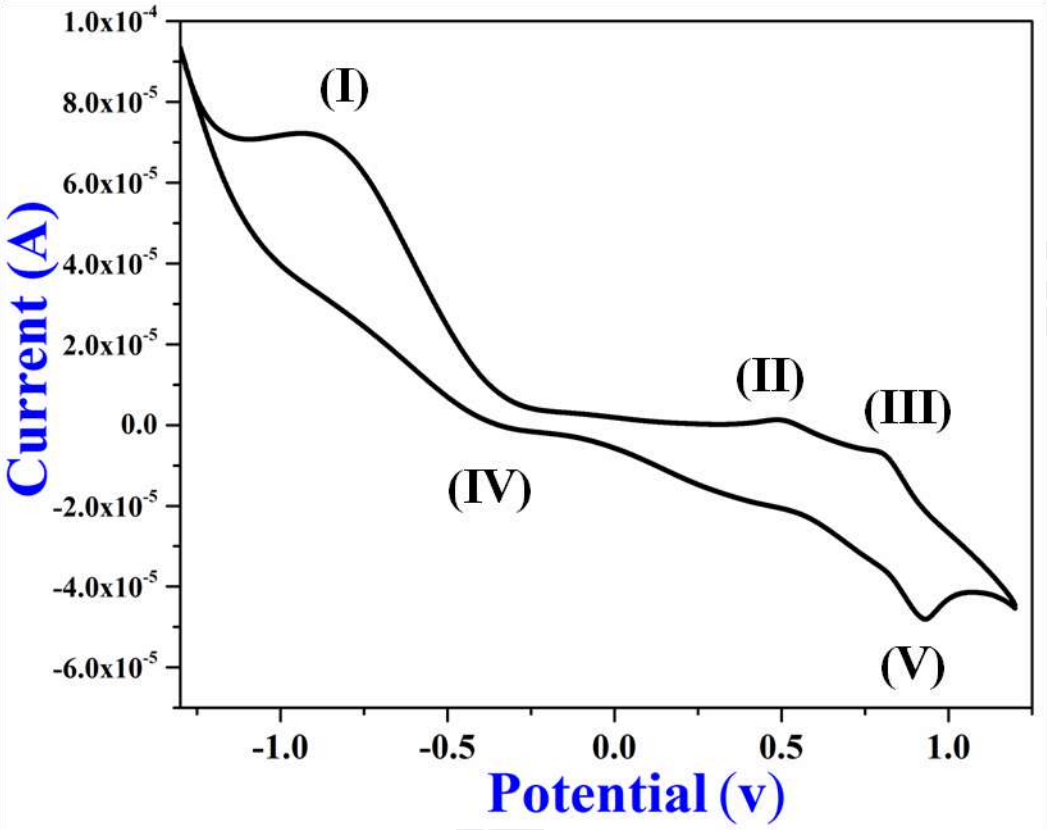

Fig. 5. Cyclic voltammograms of $[CoL_2]ClO_4$ in acetonitrile solution using a platinum working electrode in the presence of tetraethylammonium perchlorate as a supporting electrolyte at ambient temperature with scan rate 100 mV s^{-1}.

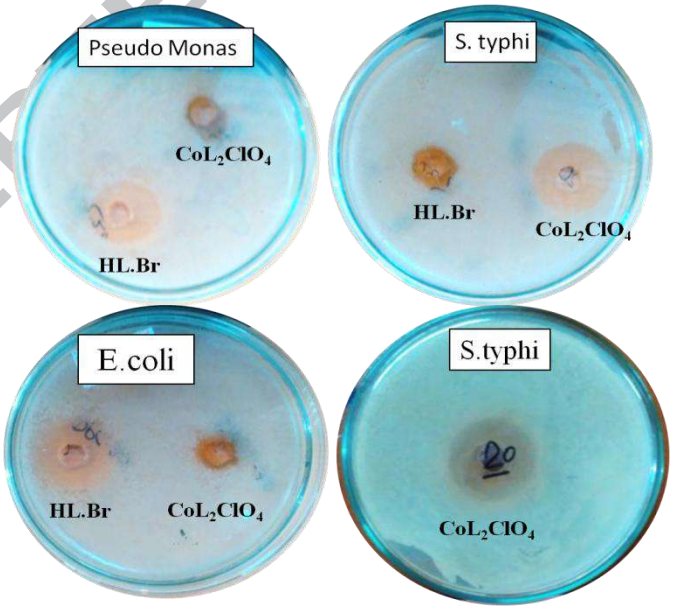

Fig. 6. Inhibition zone of ligand HL·Br and Complex $[CoL_2]ClO_4$ against *E.coli*, *Pseudo Monas* and *S. typhi* bacteria.

Synthesis of a new pyridinyl thiazole with hydrazone function and its cobalt(III) complex: X-ray crystallography, *in vitro* evaluation of antibacterial activity

Pradip Bera, Paula Brandão, Gopinath Mondal, Harekrishna Jana, Abhimanyu Jana, Ananyakumari Santra, Pulakesh Bera*

A ligand of pyridine-thiazole with hydrazone moiety and its Co(III) complex are synthesized and fully characterized by ^{1}H-NMR spectroscopy of the ligand, X-ray crystallography and cyclovoltammogram analysis. The compounds are shown to be highly active towards gram positive bacteria including *Staphylococcus aureus*, *Streptococcus fecalis* and *Bacillus subtilis* and gram-negative bacteria including *Escherichia coli*, *Pseudomonas aeruginosa*, *Salmonella Typhi*, *Klebsiella pneumonia* and *Proteus vulgaris.*